



ARTICLE

Secure Transmission of Compressed Medical Image Sequences on Communication Networks Using Motion Vector Watermarking

Rafi Ullah^{1,*}, Mohd Hilmi bin Hasan¹, Sultan Daud Khan² and Mussadiq Abdul Rahim³

¹Computer and Information Sciences Department, Universiti Teknologi PETRONAS, Bandar Seri Iskandar Perak, 32610, Malaysia

²Department of Computer Science, National University of Technology, Islamabad, 46000, Pakistan

³Interdisciplinary Research Center for Intelligent Secure Systems, King Fahd University of Petroleum and Minerals, Dammam, 31261, Saudi Arabia

*Corresponding Author: Rafi Ullah. Email: rafi.ullah@utp.edu.my

Received: 26 September 2023 Accepted: 13 December 2023 Published: 26 March 2024

ABSTRACT

Medical imaging plays a key role within modern hospital management systems for diagnostic purposes. Compression methodologies are extensively employed to mitigate storage demands and enhance transmission speed, all while upholding image quality. Moreover, an increasing number of hospitals are embracing cloud computing for patient data storage, necessitating meticulous scrutiny of server security and privacy protocols. Nevertheless, considering the widespread availability of multimedia tools, the preservation of digital data integrity surpasses the significance of compression alone. In response to this concern, we propose a secure storage and transmission solution for compressed medical image sequences, such as ultrasound images, utilizing a motion vector watermarking scheme. The watermark is generated employing an error-correcting code known as Bose-Chaudhuri-Hocquenghem (BCH) and is subsequently embedded into the compressed sequence via block-based motion vectors. In the process of watermark embedding, motion vectors are selected based on their magnitude and phase angle. When embedding watermarks, no specific spatial area, such as a region of interest (ROI), is used in the images. The embedding of watermark bits is dependent on motion vectors. Although reversible watermarking allows the restoration of the original image sequences, we use the irreversible watermarking method. The reason for this is that the use of reversible watermarks may impede the claims of ownership and legal rights. The restoration of original data or images may call into question ownership or other legal claims. The peak signal-to-noise ratio (PSNR) and structural similarity index (SSIM) serve as metrics for evaluating the watermarked image quality. Across all images, the PSNR value exceeds 46 dB, and the SSIM value exceeds 0.92. Experimental results substantiate the efficacy of the proposed technique in preserving data integrity.

KEYWORDS

Block matching algorithm (BMA); compression; full-search algorithm; motion vectors; ultrasound image sequence; watermarking



1 Introduction

The conventional aphorism “seeing is believing” has become obsolete in the era of sophisticated software and intelligent tools, facilitating inconspicuous modifications and reproductions of digital media. Consequently, it is imperative for proprietors of media content and hospital management systems to accord precedence to the secure transmission and storage of digital media, with particular emphasis on medical images, which carry heightened significance compared to other categories of multimedia information. Medical images, such as those obtained from computed tomography (CT) and positron emission tomography (PET), play a pivotal role in cancer detection. In the prior study [1], the authors introduced a cloud-based prediction model for breast cancer prediction. Similarly, another study [2] proposed a multi-class classification for breast cancer utilizing histopathological images. In related work [3], the authors enhanced the hybrid vision transformer network for cancer detection in histopathological images, demonstrating superior results in terms of F-score compared to the existing architectures.

One of the most auspicious approaches for ensuring the security of critical data involves the application of digital watermarking, a technique wherein confidential information is concealed within the cover work or medical images [4–8]. Two predominant categories of watermarking techniques are blind watermarking and informed watermarking with the latter experiencing infrequent utilization over the past two decades. In medical applications, where even minor distortions can lead to erroneous diagnoses, the preservation of visual integrity during data embedding is paramount. To address this concern, reversible watermarking techniques have been proposed, allowing for the restoration of original data or images [9–11]. However, this solution introduces legal and ethical problems, as the restoration of original data or images may impede claims of ownership or other legal rights. Furthermore, a considerable-capacity requirement of reversible watermarking constitutes a second major limitation. These issues necessitate comprehensive exploration in future research endeavors.

Watermarking is a versatile technique used for various purposes, encompassing copyright protection, authentication, copy control, transaction tracking, proof of ownership, broadcast monitoring, and legacy enhancement [12]. In the proposed watermarking methodology, we ensure the secure transmission and storage of compressed medical image sequences, specifically ultrasound, by embedding watermark bits (secret messages) in the host image sequence resulting in a watermarked image sequence. The embedded message is designed to withstand benign manipulation and adhere to robustness constraints while preserving the visual perception of the image sequence. This data can subsequently be securely transmitted via wired or wireless communication channels. To achieve this objective, we have developed an approach that involves compressing the ultrasound sequence using JPEG-LS (JPEG lossless) and head code compression (HCC) before embedding the watermark bits through motion estimation. A full-search BMA has been used for motion vector extraction.

In the realm of medical imaging and healthcare, the diagnostic process extensively relies on medical images, and sequences including those derived from computed tomography, magnetic resonance imaging and ultrasound. The transmission of such data especially over the wired or wireless networks necessitates efficient compression techniques. The challenge addressed by the proposed method lies in compressing ultrasound sequences before embedding the watermark, while preserving imperceptibility and robustness. This study endeavours to formulate a resilient embedding algorithm that upholds imperceptibility under benign interventions. This objective is accomplished by strategically selecting the size and phase angle between motion vectors for embedding. Specifically, motion vectors with high magnitude, indicative of rapid physical movements within the macroblocks, are selected for the watermark bit. Modifying high-magnitude motion vectors is less perceptible than altering lower-magnitude motion vectors [13].

This paper examines various pivotal parameters in the context of watermarking, encompassing imperceptibility, security level, robustness, and capacity [12]. In order to enhance transmission speed and reduce storage demands, we employed lossless compression techniques to compress the medical images or sequences, facilitating the recovery of the original content post-decompression [14,15]. Departing from the conventional approach that involves spatial regions of the sequence frames, we opted for leveraging temporal information watermark embedding. Section 4 is dedicated to the elucidation of the extraction process of temporal information, specifically in the form of motion vectors.

The subsequent sections of this paper are structured as follows: Section 2 furnishes a comprehensive literature review. The proposed algorithm is explicated in Section 3. Section 4 details the experimental results while Section 5 offers an in-depth discussion of the compression and motion estimation of the medical image sequence. Finally, Section 6 concludes the paper and proffers suggestions for further research endeavors.

2 Literature Survey

In previous work [16], a BMA-based method for multiresolution video watermarking was proposed. This method involves the selection of blocks characterized by large motion vectors followed by the decomposition of the frame using wavelet transform. Subsequently, the watermark is embedded within the horizontal coefficients of these blocks, resulting in a scheme that exhibits robustness against various attacks while maintaining imperceptibility. Furthermore, research efforts [17] have proposed models for both uncompressed and compressed video watermarking models. These models delve into the analysis of scalable video coding (SVC) encoder architecture. Three distinct strategies for watermarking were explored: embedding prior to video encoding, a combined embedding and coding strategy, and embedding after encoding within a compressed domain.

A compressed video watermarking technique, utilizing affine invariant regions, was proposed by [18]. Its technique proves efficacious for discrete cosine transform (DCT)-based compressed video frames and demonstrates robustness against geometric attacks. The process involves decoding frames from DCT transforms to the spatial domain, implementing a fast inter-transform within DCT blocks and sub-blocks, and obtaining 2×2 DCT blocks through downsampling the corresponding DC coefficient. Robustness assessments were conducted, specifically considering cropping and frame-rate conversion. Two decades prior, Hartung and Girod proposed a scheme for compressed and uncompressed video watermarking based on spread-spectrum communication [19] using an MPEG-2 test video. The system can embed additional information, extending from prior work with an uncompressed video. A drift compensation signal was incorporated to enhance imperceptibility. Reference [20] proposed blind video watermarking methods within a compressed domain, wherein multiple binary images are derived from the watermarked image and then embedded directly into the video sequence, incorporating the watermark bits into the four sets in the wavelet domain. In [21], the authors presented a robust watermarking method based on deep neural network (DNN) designed for high-quality compressed video. The video is compressed using the HEVC codec, aiming to ensure the watermarked video's resilience through the compression channel inherent to the HEVC codec. Another watermarking approach introduced in [22], involves motion vectors and claims to achieve favorable video quality using intra-modes for encoding macroblocks. This method allows for high video compression in certain scenarios by reducing the bit rate of the video. Motion vector watermarking has been extended to HEVC video in [23], offering dual protection of videos. This protection is realized through the embedding of watermark bits using motion vector watermarking

and scrambling all motion vectors. Reference [24] proposed inter- or intra-block motion vector watermarking maintaining superior image quality even with a high data payload, although the sensitivity to transcoding is acknowledged. Furthermore, in [25], a motion vector watermark was introduced to authenticate normal videos ensuring full protection in both the spatial domain and the transform domain. The embedding of the watermark bits relies on the magnitude and phase angle of the motion vectors, extracted from the video frames using the block-based full-search motion estimation technique.

In the context of hospital management systems, the implementation of medical image watermarking is imperative for the optimization of medical image storage and the facilitation of secure exchange between hospitals and medical specialists. Electronic patient reports and their corresponding medical images were historically shared independently with watermarking methods playing a pivotal role in guaranteeing the authenticity, security, and integrity of these images. Numerous watermarking methods have been introduced to ensure the security of medical images [26–29]. The adoption of medical watermarking yields several advantages, including diminished bandwidth and memory utilization, mitigation of separation risks, and enhanced confidentiality and security measures [30].

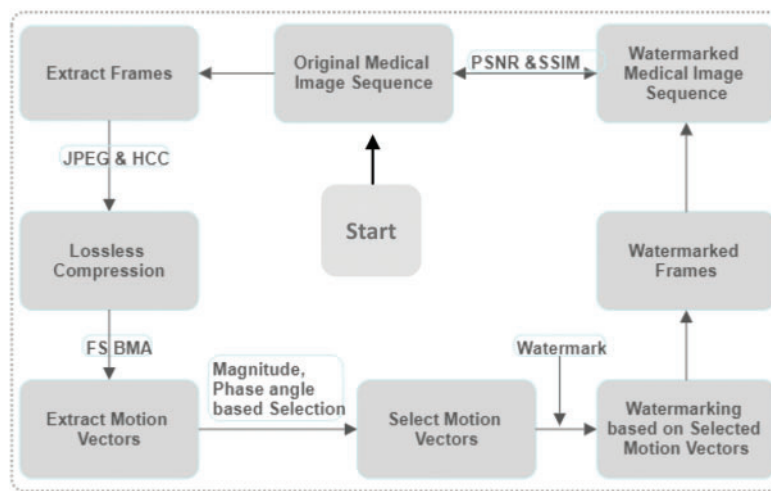
Numerous watermarking methods have been proposed in the spatial domain, involving the direct embedding of watermarks into pixels [31–35]. Since each pixel is independent, ensuring image security while preserving a high imperceptibility presents a considerable challenge. Similarly, various medical image watermarking algorithms have been proposed within the transform domain incorporating methods such as discrete Fourier transform (DFT) [36–38], DCT [39–41], discrete wavelet transform (DWT) [42–45], dual-tree complex wavelet transform (DTCWT) [46], contourlet [47], and singular value decomposition (SVD) [48].

Various watermarking techniques have been proposed to ensure the security of ultrasound images. Notably, Badshah et al. proposed a compressed watermark embedding technique [49], which involved partitioning the input image into a region of interest (ROI) and a region of non-interest (RONI) for the purpose of authentication, tamper detection, and lossless recovery of ultrasound images. The watermark creation process utilized the hash value of the ROI, embedding it into the least significant bits (LSBs) of RONI following lossless image compression. Tiwari et al. [40] proposed a multi-frame watermarking technique designed for parallel watermarking of ultrasound images, achieving enhanced efficiency through the utilization of multicore technology. Another approach leverages motion vectors derived from an Electrocardiogram (ECG) for watermark embedding in medical images, as outlined in [41]. Additionally, in [50], the authors proposed a genetic algorithm-based motion vector watermark for medical images and sequences. The transformation domain for images and the temporal domain for medical image sequences were employed to embed the watermark and the genetic algorithm enhanced imperceptibility during the embedding process. Another motion vector watermarking approach is presented in [51], where the reversible watermark is employed to protect the uncompressed ultrasound image sequence. Reversible watermarking allows for the restoration of the original content after distortion. However, drawbacks include the inability to claim the content once the original content is restored, and the associated computational costs are high.

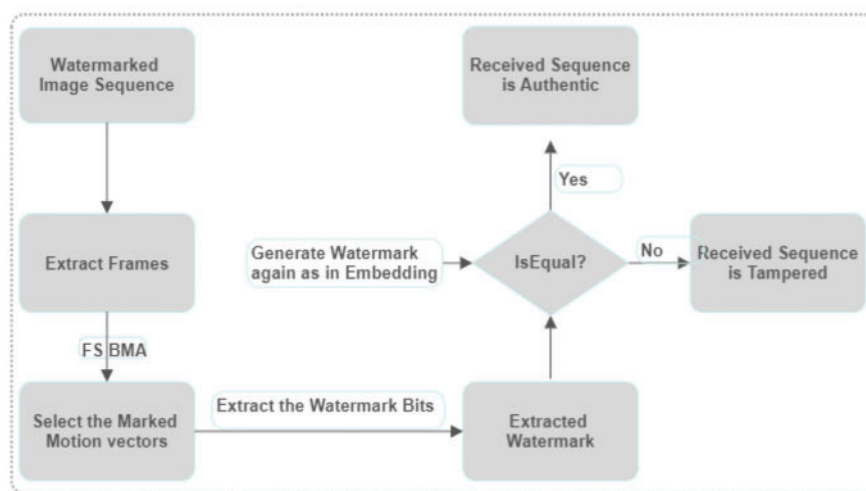
The existing literature reviewed in this section presents a plethora of solutions aimed at enhancing the security of medical images and sequences. Nonetheless, a notable gap is identified concerning the treatment of compressed medical images or sequences. In the proposed method, our approach involves the compression of the ultrasound image sequence prior to embedding the high-impact watermark. This is done with careful attention to preserving imperceptibility and ensuring robust security measures.

3 Materials and Methods

Fig. 1 illustrates the watermark embedding and extraction procedure within the context of our proposed algorithm designed for embedding watermarks in ultrasound image sequences. In this algorithm, we employ full-search (FS) BMA to obtain motion vectors due to its superior effectiveness compared to other BMAs, albeit at the cost of increased computational time. Before embedding the watermark, we subject compressed the image sequence to compression utilizing both JPEG-LS and HCC techniques. This is because most lossless compression methods are designed for single images neglecting inter-frame correlations in the image sequences [42]. The compression comprises two distinct phases: Modelling and coding. The JPEG-LS method is employed to achieve ratio of 4:8, a ratio that undergoes further enhancement through the incorporation of HCC [43]. In this context, dictionary coding and Huffman coding are used to compress the content of the JPEG-LS compressed images. The ultrasound image sequence undergoes compression in two stages: initially with JPEG-LS followed by compression with HCC. The experimental work is conducted using MATLAB software.



(a)



(b)

Figure 1: Block diagrams of (a) watermark embedding and (b) watermark extraction

3.1 Compression

The compression procedure is delineated through the following steps:

1. Individual image extraction: Images are extracted individually from ultrasound image sequences. The initial frame undergoes compression independently, lacking a reference frame, whereas subsequent frames are compressed with reference to the preceding frame.
2. Motion estimation and compensation (MEMC): MEMC is applied to both the current frame and the reference frames, the process reiterated for all frames in the sequence. MEMC encompasses three crucial steps.
 - a) Calculation of displacement vector of a single pixel or a group of pixels across frames.
 - b) Prediction of the current frame's corresponding pixel using the displacement vector.
 - c) Encoding and transmission of prediction errors, locations, and motion vectors.
3. Motion vectors are derived from two frames employing the FS algorithm, as explained in [Section 5.2](#).
4. Further compression is achieved through HCC, wherein each codeword is characterized by a head code and a tail code. The head code, represented by initial bit, serves to denote whether the current pixel matches the preceding one.
5. Codewords exclusively comprising identical pixels are equipped with a readily available head code for compression.
6. The watermark bits are generated randomly using a private key, and additional bits are incorporated to fortify the watermark through BCH encoding. This fortification enhances the watermark robustness but at the cost of less similarity between the original and the watermarked image. The BCH encoding pair (31,21,2) encompasses 21 real bits, 31 physical bits, and two corrected bits [44]. Various BCH encoding pairs are details in [Table 1](#).

Table 1: Generation of primitive BCH codes where **n** represents the actual bits, **k** represents the physical bits and **t** represents the number of bits that can be recovered after compression

N	7	15	31	63	255																			
k	4	11	7	5	26	21	16	11	6	57	51	45	39	36	171	163	155	147	139	131	123	115	107	99
t	1	1	2	3	1	2	3	5	7	1	2	3	4	5	11	12	13	14	15	18	19	21	22	23

3.2 Watermark Generation and Embedding

The subsequent procedures were executed for watermark generation and embedding.

1. The watermark bits were generated in stochastic manner employing a private key, and additional bits were incorporated to fortify the watermark through BCH encoding. This augmentation enhances the resilience of the watermark but at the cost of diminished similarity between the original and the watermarked image. The BCH encoding pair (31,21,2) contains 21 real bits, 31 physical bits, and two corrected bits [52]. Various BCH-encoding pairs are delineated in [Table 1](#).
2. The FS-BMA is deployed to extract motion vectors from the compressed image sequence.
3. The watermark is embedded in the motion vectors in a manner that impart resistance to benign manipulation.

4. Motion vectors are selected based on their magnitude, phase angle, and the corresponding macroblocks for embedding. The computation of vector magnitude and phase angles is performed using Eqs. (1) and (2).

$$|\text{Mag}_v(i)| = \sqrt{h_i^2 + v_i^2}, 0 \leq i \leq \text{MB} \quad (1)$$

where h and v are the horizontal and vertical values of the vectors, respectively; MB is the number of macroblocks, and Mag is the magnitude of the motion vector.

$$\Theta(j) = \tan^{-1} \left(\frac{v_j}{h_j} \right) \quad (2)$$

A threshold value τ is established to discern the selected motion vectors. When the bit salted for embedding is 1, coordinates from sectors I and II are chosen, while coordinates from sectors III and IV are designated as 0 for the intended bit embedding. If $0 \leq \theta \leq 90$, then the horizontal value of the chosen vector is adjusted; if $90 < \theta \leq 180$, the vertical value of the chosen vector is adjusted [53]. This iterative process is applied to all frames within the input sequence. The efficacy of the embedded bits is assessed using the PSNR as defined by Eq. (3), and the SSIM as defined by Eq. (4). SSIM serves as a perceptual metric employed to quantify the degradation of the watermarked image with its value ranging from -1 to 1 . An SSIM value of 1 indicates that the images are identical. It is noteworthy that SSIM diverges from PSNR in its utilization for gauging image similarity based on the luminance, contrast, and pixel texture. In contrast, PSNR is employed to assess degradation by considering the absolute error between pixels.

$$\text{PSNR} = 20 \log_{10} \left(\frac{255^2}{\text{MSE}} \right) \quad (3)$$

where MSE is the mean square error. The MSE is computed by using the Eq. (4).

$$\text{MSE} = \frac{1}{\text{MN}} \sum_{y=1}^M \sum_{x=1}^N [I(x, y) - I'(x, y)]^2 \quad (4)$$

where $I(x, y)$ and $I'(x, y)$ are the original and watermarked images, respectively. M and N represent the dimension of image under consideration.

$$\text{SSIM}(x, y) = \frac{(2\mu_x\mu_y + c_1)(2\sigma_{xy} + c_2)}{(\mu_x^2 + \mu_y^2 + c_1)(\sigma_x^2 + \sigma_y^2 + c_2)} \quad (5)$$

where x and y are two windows each of size $N \times N$, μ_x and μ_y denote the averages of x and y , and σ_x^2 and σ_y^2 represent the variances of x and y , respectively. $c_1 = (K_1L)^2$ and $c_2 = (K_2L)^2$ where L signifies the maximum value, i.e., $2^{\#\text{bites}}$, and default values for k_1 and k_2 are assigned as $k_1 = 0.01$ and $k_2 = 0.03$, respectively.

3.3 Watermark Extraction and Verification

The process of motion vector selection for watermark extraction mirrors the threshold-based methodology employed in the embedding phase, wherein the calculation of magnitude and phase angle is paramount. The embedded watermark bits are subsequently retrieved from the motion vectors that have been strategically chosen. At the recipient's end, the watermark is reconstructed, and comparative analysis is conducted against the extracted watermark to ascertain the genuineness of the image. The watermark verification procedure involves an examination of the phase angle of the watermarked motion vector using an analogous protocol. the ensuing steps include scrutinizing the phase angle and

the following criterion is applied: If $0 \leq \theta \leq 90$, the watermark bit is extracted from the horizontal component of the vector; conversely, if the phase angle falls in the range of $90 \leq \theta \leq 180$, the watermark bit is extracted from the vertical component. This procedural sequence is iteratively applied to all frames within the sequence.

4 Experimental Results and Discussion

Our algorithm undergoes evaluation utilizing a ten-second ultrasound sequence. The initial step involves the application of lossless compression followed by the utilization of the FS BMA to extract the motion vectors. The first quartet of the extracted frames is visually depicted in [Fig. 2](#).

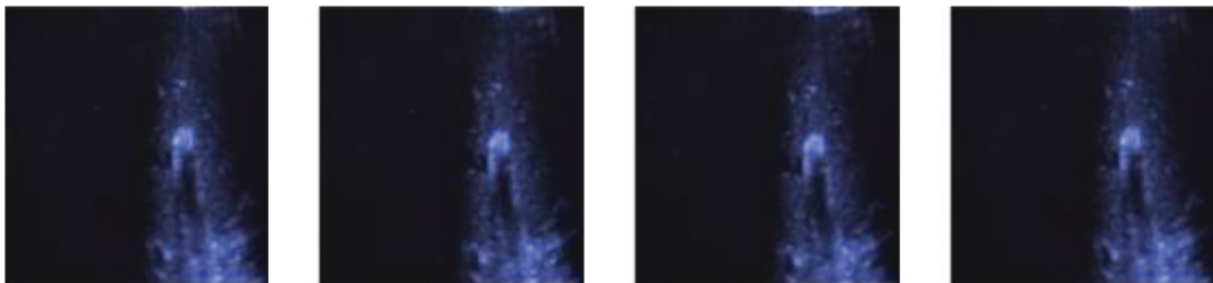


Figure 2: Four extracted frames of the compressed ultrasound video

Ultrasound image sequences exhibit a multitude of motion vectors within the initial four frames, as illustrated in [Fig. 3](#). This observation, in contrast to conventional videos, signifies the heightened complexity of medical image sequences, providing a more extensive canvas for the incorporation of watermark bits. This surplus capacity facilitates the embedding of high-strength watermarks, a requisite feature considering the security demands of medical image applications. As illustrated in [Fig. 4](#), the corresponding quartet of watermarked frames encompasses numerous motion vectors shared between adjacent frames. Consequently, effective watermark embedding is achieved through the judicious selection of appropriate motion vectors from a substantial reservoir.

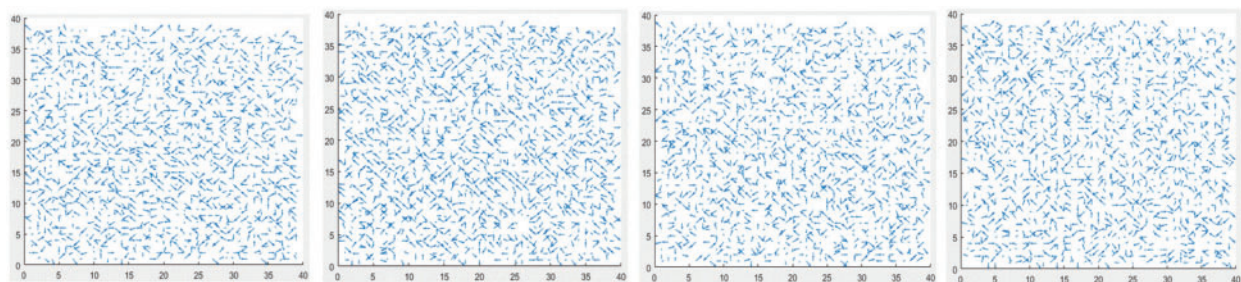


Figure 3: The motion vectors for the first four frames

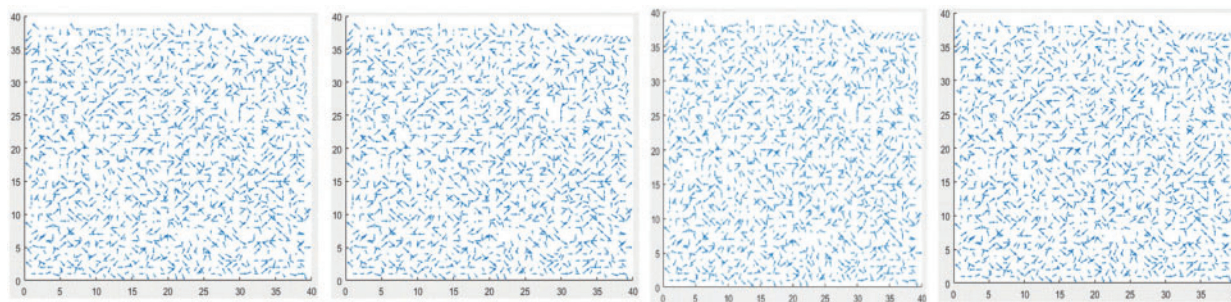


Figure 4: The watermark embedded in the motion vectors of Fig. 3

Selecting motion vectors characterized by a substantial and minimal phase angle has been facilitated in our approach as we did not incorporate ROI and RONI considerations during the watermark embedding process. It is noteworthy that the inclusion of ROI and RONI without consultation with physicians and hospital management systems poses a formidable challenge in our methodology.

Table 2 lists the PSNR and SSIM values corresponding to both the original and watermarked frames. The designated acceptable range for PSNR lies between 45 and 49 dB, while the optimal SSIM range is 1, signifying the perfect structural similarity between two identical frames. Our devised methodology has demonstrated commendable structural similarity affirming that the original frames exhibit substantial likeness to the corresponding watermarked frames. Our proposed method facilitates the sharing and storage of ultrasound images by enabling the recovery of altered locations achieved through the utilization of a BCH encoder and decoder. Comprehensive details of BCH pair combinations are enlisted in Table 1.

Table 2: Perceptual and structural similarity for the selected four frames

Frame number	PSNR	SSIM
1	47.12	0.95
2	46.46	0.94
3	48.01	0.92
4	46.92	0.95

Ensuring the security of medical images and sequences necessitates the incorporation of a secret during the watermark creation process. After the image sequence is received, a verification process is imperative at the receiving end. The visual representation of motion vectors obtained through the application of both correct and incorrect keys is depicted in Fig. 5.

Fig. 6 presents the histogram of the 15th frame within the ultrasound image sequence, along with the corresponding frames containing watermarks. The observed similarity between the histograms of both the original and watermarked frames implies the efficacy of the proposed method preserving the visual quality of the watermarked frame. The distinct ultrasound sequence is employed for the purpose of histogram analysis. Similarly, Fig. 7 provides a visualization of PSNR and SSIM values for the initial fifty frames. The recorded PSNR and SSIM values validate the performance exhibited by the proposed method.

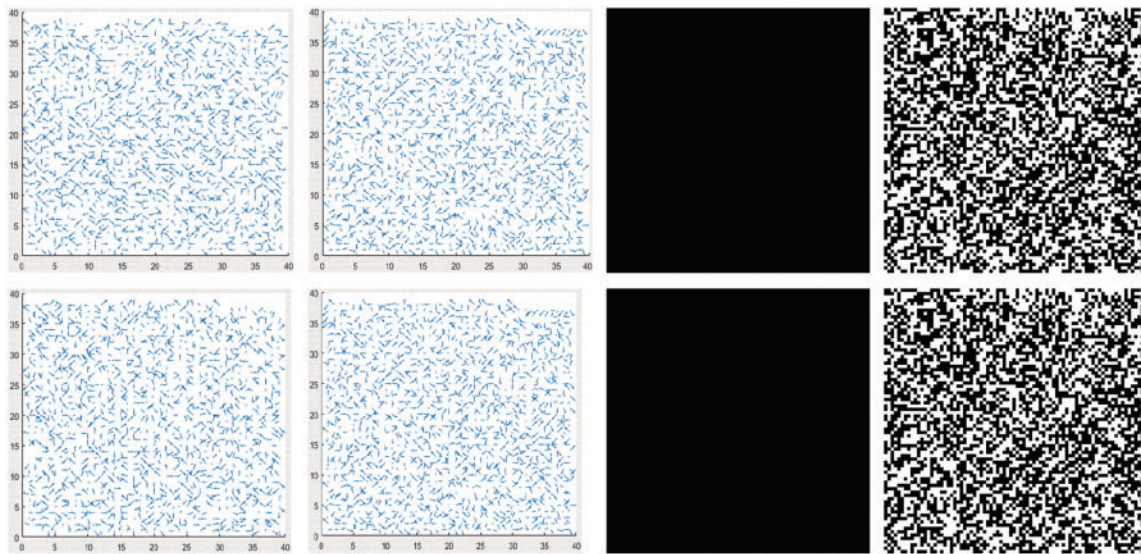


Figure 5: The first and second columns show the original and watermarked motion vectors of the first and fourth frames, respectively. The third and fourth columns show the differences between the original and extracted watermarks utilizing the correct and incorrect keys, respectively

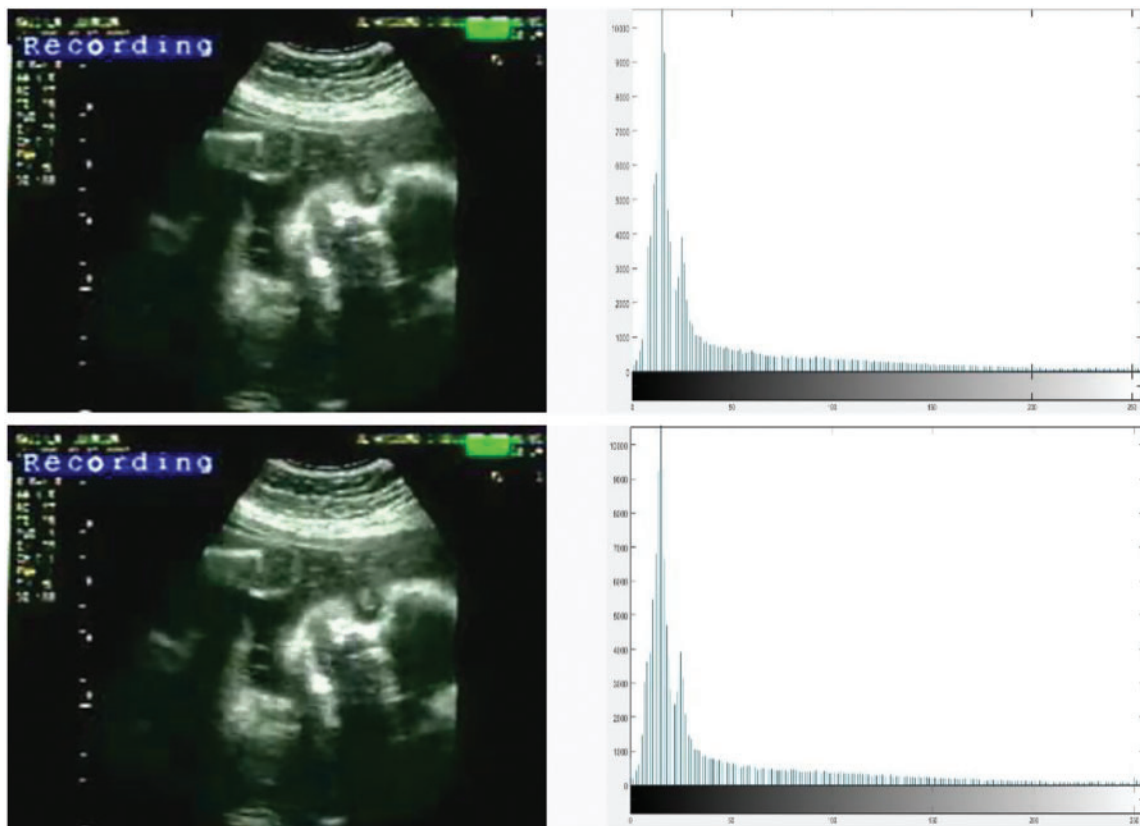


Figure 6: Column 1: Original and watermarked frames. Column 2 histogram of the original and watermarked frames

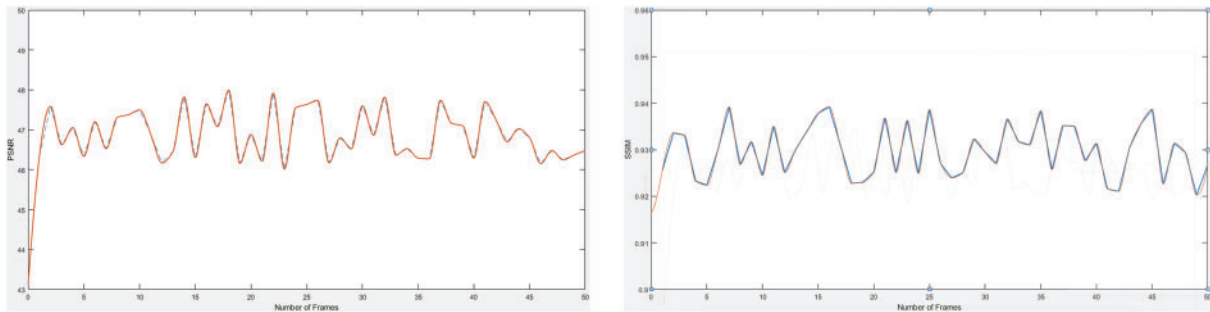


Figure 7: Shape-preserving PSNR and SSIM for first fifty frames

Table 3 provides a comparative analysis between the proposed technique and the references [54,55]. It is noteworthy that a lack of research exists in the literature, specifically pertaining to the embedding of a watermark in the compressed version of an ultrasound image sequence. Instead, the proposed technique is compared to [54,55], wherein the authors proposed watermarking techniques designed for uncompressed medical images. The comparison is predicted on visual perception, employing the PSNR and SSIM as metrics to quantify image distortion after watermark embedding. As reported in [54], the average PSNR for various medical images, encompassing CT, MRI, brain, and ultrasound images, is established at 36 dB. In contrast, the proposed scheme attains an average PSNR value of 47 dB for the four frames comprising the ultrasound image sequence. Similarly, reference [55] undertook watermark embedding in uncompressed ultrasound images, employing solely PSNT as a metric to assess image distortion.

Table 3 : Performance comparison of the proposed technique with [54] and [55]

	[54]	[55]	Proposed
Compressed?	No	No	Yes
PSNR	Average: 36 dB	Average: 47 dB	Average: 47 dB
SSIM	Nil	Nil	Average: 0.94

5 Discussion

The advent of social networks, exemplified by platforms like Facebook, Twitter, and Instagram has significantly facilitated the accessibility and distribution of multimedia content. However, this convenience has brought forth challenges related to unauthorized downloading, copying, and manipulation of digital content, emphasizing need for robust security measures. Over the past three decades, researchers' endeavors have concentrated on the deployment of multimedia watermarks to ensure the security and authentication of digital content. notably, the realm of medical images presents unique challenges due to the intricate interplay between imperceptibility and capacity of watermark that unfortunately lack precise definitions of in existing literature, leading to practical ambiguities. Another notable research gap pertains to the determination of security levels. Despite these challenges, researchers have developed various models to protect medical images employing varied watermark types such as signatures, binary codes, or secret information. Blind methods which operate without requiring access to the original content have gained prominence. Watermarking techniques can be implemented across transformed, spatial, or temporal domains. Spatial domain modifications

involve direct alterations to image pixels for embedding watermark bits, whereas transformed domain modifications utilize frequencies like DCT, DFT, and FFT for the embedding process [56,57].

The consideration of imperceptibility, robustness, and watermark payload represents a critical tradeoff within the domain of watermarking. Imperceptibility characterizes the visual similarity between the original and watermarked images, while robustness quantifies the watermarked image's resilience against attacks and various image processing operations. Capacity pertains to the volume of information that can be embedded in one or more images, with medical image sequences typically exhibiting greater embedding capacities compared to conventional video. Security encompasses the reliability of a watermarking system in instances where an attacker employs watermarking techniques without knowing the secret key used for watermarking the images. Regrettably, extinct literature inadequately addresses this issue, and most existing systems generally lack well-defined security levels. Achieving an optimal tradeoff necessitates a watermarking system that effectively balances imperceptibility, robustness, and watermark payload [58].

5.1 Compression of Medical Images and Sequences

Hospital management systems are required to effectively handle extensive volumes of medical data encompassing diverse modalities such as X-ray, CT, MRI, and ultrasound images. This presents notable challenges in terms of storage and transmission. In the present work, lossless compression approach is employed for the processing of medical images and sequences prior to their archival. This is motivated by the impermissibility of data loss associated with lossy techniques, such as JPEG compression, within the context of medical imaging applications. The utilization of lossless compression guarantees reversibility and complete recovery of original images without any compromise in data integrity [59].

Rai et al. employed MPEG coding in their study to augment storage capacity with minimal impact [60]. Their approach involved the utilization of block-based motion estimation to mitigate temporal redundancies in videos. Furthermore, they introduced a lossless compression method employing set partitioning in the hierarchical tree and motion estimation. This method yielded 37% improvement compared to the lossy JPEG compression technique [61]. Monika et al. proposed a random permutation coefficient algorithm for compressing medical images using sparsity considerations. Specifically, they identified strongly correlated pixels within the block as strongly sparse when located near each other, and weakly sparse otherwise [62]. A previous proposal focused on leveraging the unique properties of ultrasound for the compression of ultrasound image sequences [63]. The authors asserted the achievement of specialized compression and transport of ultrasound images, a feature that is not present in the existing systems. Another recent compression method was introduced, which is based on computing the shared information between high-contrast regions in medical images [64].

Proceeding the embedding of the watermark, the methodology of lossless compression, specifically founded on motion estimation and Huffman coding described in [Section 3.1](#). This approach delineates a comprehensive process for compressing medical images, facilitating the minimization of storage demands and acceleration of transmission speed.

5.2 Motion Estimation

Motion estimation constitutes a process applied in video compression and analysis to ascertain the motion of entities between consecutive video frames. This procedure involves the comparison of two or more frames within a video sequence and the computation of motion vector, which signifies the displacement of an object or a set of pixels across frames. While motion estimation in the medical

image sequences shared similarities with its counterpart in normal videos, distinction arise due to the distinctive nature of medical images. In medical image sequences, the primary objective is to appraise the motion of internal organs or structures within the body, subject to influences such as breathing, heartbeat, or other physiological processes. Notably, medical image sequences may exhibit characteristics such as a lower frame rate, heightened noise levels, and reduced contrast in contrast to typical video sequences, potentially impacting the precision of motion estimation.

Given the crucial role of motion estimation in medical image sequences for diverse applications including image registration, image fusion, and motion correction, it serves as a pivotal component for embedding watermark bits. Motion vectors, integral to this process, are derived through BMAs and pixel-recursive algorithms (PRAs). BMAs, characterized by computational simplicity, prove suitable for implementation in basic hardware, whereas pixel-based PRAs are inherently more complex. The motion vectors produced by BMAs furnish temporal information, and their magnitude and phase angle contribute to the identification of appropriate vectors for watermark embedding. The selection of motion vectors is contingent upon associated macroblocks, as motion vectors with substantial magnitudes may not consistently align with optimal choices for watermark embedding. Hence, careful consideration of pertinent macroblocks is conducted concurrently. The impact of watermark embedding was assessed through metrics such as peak signal-to-noise ratio (PSNR), weighted PSNR, image fidelity, and the structural similarity index (SSIM). The watermark robustness is gauged via accuracy rate, bit error rate, and correlation coefficient assessments. Numerous block-based motion-estimation algorithms, including some discussed subsequently have been documented in the literature.

5.2.1 Exhaustive Search/Full Search (ES/FS)

Despite the substantial computational effort associated with the ES/FS method, necessitating the computation of the cost function for each point within the designated window, its adoption was deemed necessary owing to its capacity for precise motion vector calculation. This BMA seeks the nearest match in the reference frame for each non-overlapping block within the current frame [56].

5.2.2 Three-Step Search (TSS)

The BMA initially proposed by Koga et al. in 1981, is a highly efficient method characterized by its approach of selecting eight adjacent blocks for comparison. In this method, a step size is divided into two parts, and the centre point is iteratively shifted to the location with the least distortion. This iterative process continues until the step size diminishes to a value less than one. Despite its efficiency, it is noteworthy that this method may exhibit limitations in accurately detecting small movements within video sequences [57].

5.2.3 New Three-Step Search (NTSS)

In mitigating the challenge of smaller movements, a novel approach known as a three-step search (NTSS), is introduced. NTSS employs a center-biased checking-point pattern during its initial step, resulting in a reduction in computational complexity and an enhancement in performance when compared to the conventional three-step search (TSS). Notably, NTSS finds widespread application in MPEG-1 and H.261 [65].

5.2.4 Four-Step Search (FSS)

The initial step involves the selection of a step size of two along with the identification of nine points arranged in a circular pattern around the center point within the search window. Subsequently,

an assessment is conducted to ascertain the direction exhibiting the least distortion. If a particular point is determined as the centre of the search area, the step size is subsequently reduced to one, and a corresponding examination of nine points ensues [66].

5.2.5 Diamond Search (DS)

Similar to FS, the DS employed a diamond-shaped search pattern; however, it differs by employing an unrestricted number of steps. Functionally akin to the NTSS, DS operates with a reduced computational cost. Additionally, DS demonstrates a significantly lower mean square error (MSE) in comparison to FSS, necessitating only a limited number of search points [67].

5.2.6 Two-Dimensional Logarithmic Search (TDLS)

Despite its increased number of steps, TDLS surpasses TSS in accuracy, particularly when larger search windows are employed. TDLS strategically select four adjacent blocks surrounding the initial central block and executes a search to identify the optimal match. The reduction in step size prompts TDLS progressively extend the search to the neighbouring blocks until the step size reaches one. Subsequently, an exhaustive assessment of all neighbouring blocks is conducted to select the most suitable match [68].

5.2.7 Orthogonal Search Algorithm (OSA)

OSA represents a hybridization of TDLS and TSS techniques. This methodology incorporates the utilization of two points positioned at a predetermined horizontal distance from the search area for the purpose of comparison, facilitating the identification of the point with the least distortion. The center point is subsequently relocated to this identified point, and the iterative process is repeated, employing a constant vertical step size until the step size diminishes to a value less than 1 [69].

In Table 4, a comprehensive performance comparison is presented for various BMAs, encompassing assessment of both frame quality and computational complexity. The second column delineates the complexities, where the parameter “p” representing the number of search points. The comparative analysis serves as a valuable resource for selecting a BMA tailored to specific application. Furthermore, the evaluation predicted frame quality for diverse BMAs is conducted using metrics such as SSIM and PSNR, the result of which are presented for comprehensive comparison.

Table 4: Comparative performance of BMAs is discussed in Section 5.2

BMA	Complexity	Advantages	Disadvantages	Comments
ES/FS	$(2 * p + 1)^2$	Give better imperceptibility	It has a higher complexity than other BMAs	FS can be used if we can ignore computational complexity
TSS	$[1 + 8 \log_2 (p + 1)]$	The complexity is low and is better for MPEG2	Not efficient against small motions	Only FS is used in our algorithm. We need the best results in terms of quality
NTSS	$[1 + 8 \log_2 (p + 1)] + 8$	The complexity is low for small motions vectors	Complexity is high as compared to TSS	

(Continued)

Table 4 (continued)

BMA	Complexity	Advantages	Disadvantages	Comments
FSS	$(18 \log_2 [(p + 1) / 4] + 9)$	The complexity is low for the low motion because of the reduced step size	Complexity is high as compared to TSS	
DS		Better than FSS in terms of MSE and search points	Like NTSS	
TDLS	$[1 + 6 \log_2 (p + 1)]$	Less complex than TSS	More suitable for highly textured frames	
OSA	$[1 + 4 \log_2 (p + 1)]$	Similar complexity to TDLS	Inefficient for small motions	

6 Conclusions and Future Work

The approach elucidated in this study employs motion vector watermarking to guarantee the confidentiality and authenticity of ultrasound image sequences. In the pursuit of optimizing the storage space and enhancing transmission speed, a dual compression strategy involving JPEG-LS and HCC lossless compression techniques is implemented prior to watermark embedding. The MEMC algorithm is employed to compress all frames through a full-search BMA technique, facilitating the extraction of motion vectors. Subsequently, appropriate vectors are selected for embedding the watermark. The HCC algorithm contributes supplementary compression, allowing for the retrieval of original images after decompression. The effectiveness of the proposed methodology is affirmed through experimental results.

In forthcoming developments, machine-learning techniques will be applied to judiciously determine suitable motion vectors for watermark embedding, guided by imperceptibility as a loss function. Furthermore, there is no need to delve into the properties and security aspects of watermarking specifically tailored for medical imaging applications. Preceding the watermark embedding process, a machine-learning-based quantization module can be implemented to achieve optimal compression of medical images and videos.

Acknowledgement: The authors would like to thank the journal editors and the reviewers for their valuable inputs during the review process of the paper.

Funding Statement: The current work was supported by the Yayasan Universiti Teknologi PETRONAS Grants, YUTP-PRG (015PBC-027) and YUTP-FRG (015LC0-311), Hilmi Hasan, www.utp.edu.my.

Author Contributions: Conceptualization was conducted by Rafi Ullah and Sultan Daud Khan; the methodology was developed by Rafi Ullah and Sultan Daud Khan; software development involved Rafi Ullah, Sultan Daud Khan, and Hilmi bin Hasan; the validation procedures were executed by Sultan Daud Khan, Mohib Ullah, and Hilmi bin Hasan; formal analysis was undertaken by Sultan Daud Khan and Hilmi bin Hasan; the original draft was prepared by Rafi Ullah; review

and editing were conducted by Sultan Daud Khan and Mussadiq Abdul Rahim; visualization tasks were performed by Rafi Ullah and Hilmi bin Hasan. All the authors have thoroughly reviewed and consented to the submission of the manuscript for publication.

Availability of Data and Materials: The data that support the findings of this study are openly available in <https://paperswithcode.com/dataset/us-4>.

Conflicts of Interest: The authors declare that they have no conflicts of interest to report regarding the present study.

References

- [1] K. Pathoee, D. Rawat, A. Mishra, V. Arya, M. Kuchal and A. K. Gupta, "A cloud-based predictive model for the detection of breast cancer," *Int. J. Cloud Comput. (IJCAC)*, vol. 12, no. 1, pp. 1–12, 2022. doi: 10.4018/IJCAC.310041.
- [2] S. Tummala, J. Kim, and S. Kadry, "BreaST-Net: Multi-class classification of breast cancer from histopathological images using ensemble of swin transform, mathematics," *Math.*, vol. 10, pp. 2–15, 2022.
- [3] M. Liaqat, Z. Rauf, A. Khan, A. Sohail, R. Ullah and J. Gwak, "CB-HVT Net: A channel-boosted hybrid vision transformer network for lymphocyte detection in histopathological images," *IEEE Access*, vol. 11, pp. 115740–115750, 2023. doi: 10.1109/ACCESS.2023.3324383.
- [4] K. Fares, K. Amine, K. Redouane, and E. Salah, "A DWT based watermarking approach for medical image protection," *J. Amb. Intel. Hum. Comp.*, vol. 12, no. 2, pp. 2931–2938, 2021. doi: 10.1007/s12652-020-02450-9.
- [5] Z. Narima, K. Amine, K. Redouane, K. Fares, and E. Salah, "A DWT-SVD based robust digital watermarking for medical image security," *Forensic Sci. Int. Elsevier*, vol. 320, pp. 110691, 2021. doi: 10.1016/j.forsciint.2021.110691.
- [6] K. Vijay, K. Pallaw, S. Udham, K. Ankit, S. Teekam and C. Swarup, "A robust medical image watermarking scheme based on nature-inspired optimization for telemedicine applications," *Electronics*, vol. 12, no. 2, pp. 882–897, 2023. doi: 10.3390/electronics12020334.
- [7] S. S. Rishi Sinhal, I. A. Ansari, and V. Bajaj, "Multipurpose medical image watermarking for effective security solutions," *Multimed. Tools Appl.*, vol. 81, pp. 1445–1463, 2022. doi: 10.1007/s11042-022-12082-0.
- [8] K. F. K. Amine, K. M. Redouane, and E. Salah, "Medical image watermarking for telemedicine application security," *J. Circuits, Syst. Comput.*, vol. 31, no. 5, pp. 125133, 2022. doi: 10.1142/S0218126622500979.
- [9] H. Y. Lee, "Adaptive reversible watermarking for authentication and privacy protection of medical records," *Multimed. Tools Appl.*, pp. 1–18, 2019. doi: 10.1007/s11042-019-7322-0.
- [10] K. J. Giri, J. Zubair, and I. Javaid, "Survey on reversible watermarking techniques for medical images," in *Multimedia Security*. Singapore: Springer, 2021, pp. 177–198.
- [11] V. M. Malayila and V. Masilamani, "A novel image scaling based reversible watermarking scheme for secure medical image transmission," *ISA Trans.*, vol. 108, no. 6, pp. 269–281, 2021. doi: 10.1016/j.isatra.2020.08.019.
- [12] Kalker, I. Cox, M. Miller, J. Bloom, and J. F. Ton, *Digital Watermarking and Steganography*. UK: Elsevier, 2007.
- [13] J. Zhang, H. Maitre, J. Li, and L. Zhang, "Embedding watermark in MPEG video sequence," in *IEEE Fourth Workshop on Multimedia Signal Processing*, Cannes, France, 2001.
- [14] M. Raza, A. Adnan, M. Sharif, M. Sharif, and S. W. Haider, "Lossless compression method for medical image sequences using super-spatial structure prediction and inter-frame coding," *J. Appl. Res. Technol.*, vol. 10, no. 4, pp. 618–622, 2012. doi: 10.22201/icat.16656423.2012.10.4.386.
- [15] H. C. Kuo and Y. L. Lin, "A hybrid algorithm for effective lossless compression of video display frames," *IEEE Trans. Multimedia*, vol. 14, no. 3, pp. 500–509, 2012. doi: 10.1109/TMM.2012.2191945.

- [16] K. S. A. Mostafa and A. Ali, "Multiresolution video watermarking algorithm exploiting the block-based motion estimation," *J. Inf. Secur.*, vol. 7, no. 4, pp. 260–268, Jul. 2016. doi: 10.4236/jis.2016.74021.
- [17] N. M. Favorskaya, "Watermarking models of video sequences," in *Computer Vision in Control Systems*. Switzerland: Springer, 2020, pp. 63–76.
- [18] H. Ling, L. Wang, F. Zou, Z. Lu, and P. Li, "Robust video watermarking based on affine invariant regions in the compressed domain," *J. Signal Process.*, vol. 91, no. 8, pp. 1863–1875, 2011. doi: 10.1016/j.sigpro.2011.02.009.
- [19] F. Hartung and B. Girod, "Hartung, an watermarking of uncompressed and compressed video," *J. Signal Process.*, vol. 66, no. 3, pp. 283–301, 1998. doi: 10.1016/S0165-1684(98)00011-5.
- [20] N. M. Sakib, D. S. Gupta, and N. S. Biswas, "A robust DWT-based compressed domain video watermarking technique," *Int. J. Image Graph.*, vol. 20, no. 1, pp. 1–18, 2020.
- [21] M. K. Piotrowski and Zbigniew, "High-quality video watermarking based on deep neural networks and adjustable subsquares properties algorithm," *Sensors*, vol. 22, no. 14, pp. 1–21, 2022.
- [22] P. Wang, Z. Zheng, and L. Li, "A video watermarking scheme based on motion vectors and mode selection," in *IEEE Int. Conf. Computer Sci. Softw.*, Hubei, China, 2008.
- [23] D. Roukaya, D. Salah, E. Majdi, and Z. Abdelkrim, "New hardware static and reconfigurable architectures for video watermarking system," *J. Circuits, Syst. Comput.*, vol. 29, no. 10, pp. 1–31, 2020. doi: 10.1142/S0218126620501686.
- [24] T. Kim, K. Park, and Y. Hong, "Video watermarking technique for H.264/ AVC," *Opt. Eng.*, vol. 51, no. 4, pp. 047402, 2012. doi: 10.1117/1.OE.51.4.047402.
- [25] R. Ullah, S. Khan, M. Ullah, F. Al-Macho, and H. Ullah, "Towards authentication of videos: Integer transform based motion vector watermarking," *IEEE Access*, vol. 10, pp. 75063–75073, 2022. doi: 10.1109/ACCESS.2022.3191667.
- [26] S. H. Alshanbari, "Medical image watermarking for ownership & tamper detection," *Multimed. Tools Appl.*, vol. 80, no. 11, pp. 16549–16564, 2021. doi: 10.1007/s11042-020-08814-9.
- [27] K. Priyank and K. V. Srivastava, "A secured and robust medical image watermarking approach for protecting integrity of medical images," *Trans. Emerg. Telecommun. Technol.*, vol. 32, no. 2, pp. 1–17, 2020.
- [28] K. Fares, K. Amine, K. Redouane, and E. Salah, "A robust blind medical image watermarking approach for telemedicine applications," *Clust. Comput.*, vol. 24, pp. 2069–2082, 2021. doi: 10.1007/s10586-020-03215-x.
- [29] A. Puvvadi and V. P. V. Kishore, "A blind medical image watermarking for secure e-healthcare application using crypto-watermarking system," *J. Intell. Systems*, vol. 29, no. 1, pp. 1558–1575, 2020.
- [30] S. M. Mousavi, A. Naghsh, and S. A. Abu-Bakar, "Watermarking techniques used in medical images: A survey," *J. Digit. Imaging*, vol. 27, no. 6, pp. 714–729, 2014. doi: 10.1007/s10278-014-9700-5.
- [31] X. Zhang, Q. Su, and H. Wang, "A blind color image watermarking algorithm combined spatial domain and SVD," *Int. J. Intell. Syst., Wiley*, vol. 37, no. 8, pp. 4747–4771, 2021. doi: 10.1002/int.22738.
- [32] M. Ali, "Robust image watermarking in spatial domain utilizing features equivalent to SVD transform," *Appl. Sci.*, vol. 13, no. 10, pp. 1–20, 2023.
- [33] Q. Su and H. Wang, "A color image watermarking method combined QR decomposition and spatial domain," *Multimed. Tools Appl.*, vol. 81, no. 26, pp. 37895–37916, 2022. doi: 10.1007/s11042-022-13064-y.
- [34] V. Paul and J. Abraham, "An imperceptible spatial domain color image watermarking scheme," *J. King Saud Univ.-Comput. Inf. Sci.*, vol. 31, no. 1, pp. 125–133, 2019. doi: 10.1016/j.jksuci.2016.12.004.
- [35] Z. Yuan, Q. Su, D. Liu, X. Zhang, and T. Yao, "Fast and robust image watermarking method in the spatial domain," *IET Image Process.*, vol. 14, no. 15, pp. 3829–3838, 2021. doi: 10.1049/iet-ipr.2019.1740.
- [36] M. Cedillo-Hernandez, F. Garcia-Ugalde, M. Nakano-Miyatake, and H. Perez-Meana, "Robust watermarking method in DFT domain for effective management of medical imaging," *Signal Image Video Process.*, vol. 9, no. 5, pp. 1–16, Jul. 2013. doi: 10.1007/s11760-013-0555-x.
- [37] R. E. C. H. Arevalo-Ancona and Manuel, "Zero-watermarking for medical images based on regions of interest detection using K-means clustering and discrete fourier transform," *Int. J. Adv. Comput. Sci. Appl.*, vol. 14, no. 6, pp. 581–588, 2023. doi: 10.14569/issn.2156-5570.

- [38] H. J. Cao, F. X. Hu, Y. H. Sun, S. Y. Chen, and Q. T. Su, "Robust and reversible color image watermarking based on DFT in the spatial domain," *Optik*, vol. 262, pp. 1–17, 2022.
- [39] M. A. Sajeer and Mishra, "A DCT-based robust and secured dual watermarking approach for color medical scans with joint permutation and diffusion encryption," *Multimed. Tools Appl.*, vol. 81, no. 6, pp. 2073, 2023. doi: 10.1007/s11042-023-17287-5.
- [40] A. Tiwari, D. Awasthi, and V. K. Srivastava, "Image security enhancement to medical images by RDWT-DCT-Schur decomposition-based watermarking and its authentication using BRISK features," *Multimed. Tools Appl., Springer*, vol. 82, no. 6, pp. 1594, 2023. doi: 10.1007/s11042-023-15878-w.
- [41] C. Zeng *et al.*, "Multi-watermarking algorithm for medical image based on KAZE-DCT," *J. Amb. Intel. Hum. Comp.*, vol. 13, no. 3, pp. 1–9, 2022.
- [42] S. H. Devi and M. Hitesh, "A novel robust blind medical image watermarking using rank-based DWT," *Int. J. Inf. Technol.*, vol. 15, no. 4, pp. 1901–1909, 2023. doi: 10.1007/s41870-023-01234-6.
- [43] K. R. M. B. Khaldi Amine, "A redundant wavelet based medical image watermarking scheme for secure transmission in telemedicine applications," *Multimed. Tools Appl.*, vol. 82, no. 5, pp. 7901–7915, 2023. doi: 10.1007/s11042-022-13649-7.
- [44] M. S. Moad, M. R. Kafi, and A. Khaldi, "A wavelet based medical image watermarking scheme for secure transmission in telemedicine applications," *Microprocess. Microsyst., Elsevier*, vol. 90, pp. 1–10, 2022.
- [45] W. Z. X. Zhang, W. Sun, X. Sun, and S. K. Jha, "A robust 3-D medical watermarking based on wavelet transform for data protection," *Computer Systems Sciene and Engineering*, vol. 41, no. 3, pp. 1043–1056, 2022.
- [46] I. W. Selesnick, R. G. Baraniuk, and N. C. Kingsbury, "The dual-tree complex wavelet transform," *Signal Process. Mag.*, vol. 22, no. 6, pp. 123–151, 2005. doi: 10.1109/MSP.2005.1550194.
- [47] F. Rahimi and H. Rabbani, "A dual adaptive watermarking scheme in contourlet domain for DICOM images," *BioMed. Eng. OnLine*, vol. 10, no. 1, pp. 1–18, 2011. doi: 10.1186/1475-925X-10-53.
- [48] A. Dey, P. Chowdhuri, P. Pal, and T. Z. Lu, "SVD-based watermarking scheme for medical image authentication," in *Proc. Int. Conf. Netw. Secur. Blockchain Technol.*, Midnapur, India, 2023.
- [49] G. Badshah, S. C. Liew, J. M. Zain, and M. Ali, "Watermarking of ultrasound medical images in teleradiology using compressed watermark," *J. Med. Imaging*, vol. 3, no. 1, pp. 01700-1–01700-10, 2016. doi: 10.1117/1.JMI.3.1.017001.
- [50] H. Alquhayz and B. Raza, "Watermarking techniques for the security of medical images and image sequences," *Arab. J. Sci. Eng.*, vol. 47, no. 8, pp. 9471–9488, 2022. doi: 10.1007/s13369-021-06254-7.
- [51] R. Ullah and F. Al-Fayez, "Protection of ultrasound image sequence: Employing motion vector reversible watermarking," *Int. J. Adv. Comput. Sci. Appl.*, vol. 10, no. 4, pp. 141–149, 2019.
- [52] J. G. Wade, *Signal Coding and Processing*, 2nd ed. UK: Cambridge University Press, 1994.
- [53] R. Ullah and H. Alquhayz, "Authentication of topographic EEG: Employing transform based watermarking," *Int. J. Comput. Sci. Netw. Secur.*, vol. 17, no. 3, pp. 43–54, 2017.
- [54] A. K. Singh, M. Dave, and A. Mohan, "Hybrid technique for robust and imperceptible multiple watermarking using medical images," *Multimed. Tools Appl.*, vol. 75, no. 14, pp. 8381–8401, Jul. 2016.
- [55] H. L. Khor, S. C. Liew, and J. M. Zain, "Parallel digital watermarking process on ultrasound medical images in multicores environment," *Int. J. Biomed. Imaging*, vol. 2016, pp. 1–14, 2016. doi: 10.1155/2016/9583727.
- [56] H. Y. Ding, Y. J. Zhou, Y. Yang, and R. Zhang, "Robust blind video watermark algorithm in transform domain combining with 3D video correlation," *J. Multimed.*, vol. 8, no. 2, pp. 161–167, 2013. doi: 10.4304/jmm.8.2.161-167.
- [57] O. S. Faragallah, "Efficient video watermarking based on singular value decomposition in the discrete wavelet transform domain," *AEU–Int. J. Electron. Commun.*, vol. 67, no. 3, pp. 189–196, Mar 2013. doi: 10.1016/j.aeue.2012.07.010.
- [58] H. Tao, L. Chongmin, J. Mohamad Zain, and A. N. Abdalla, "Robust image watermarking theories and techniques: A review," *J. Appl. Res. Technol.*, vol. 12, no. 1, pp. 122–138, Feb 2014. doi: 10.1016/S1665-6423(14)71612-8.

- [59] M. F. Ukrit and G. R. Suresh, "Lossless compression for medical image sequences using combination methods," in *2nd National Conf. Comput. Intell. Electr. Electron. Eng.*, Chennai, India, 2013, pp. 14–18.
- [60] J. K. Rai, and C. Kumargaonkar, "Medical image sequence compression using motion compensation and set partitioning in hierarchical trees," *Res. J. Eng. Sci.*, vol. 5, no. 4, pp. 20–25, 2016.
- [61] M. Sharma, C. Kamargaonkar, and J. K. Rai, "Medical image sequence compression using fast block matching algorithm and SPIHT," in *3rd Int. Conf. Comput. Sustain. Global Dev.*, New Dehli India, 2016.
- [62] R. Monika, S. Dhanalakshmi, and S. Sreejith, "Coefficient random permutation based compressed sensing for medical image compression," in *Advances in Electronics, Communication and Computing*, Singapore: Springer, 2017, pp. 529–536.
- [63] A. Matani, H. Yagi, T. Umeda, and K. Chihara, "A compression and transmission system of ultrasonic image sequence for telemedicine," *Telemed. J.*, vol. 5, no. 4, pp. 385–389, 1999. doi: 10.1089/107830299311952.
- [64] L. H. Lin and T. J. Chen, "Mutual information correlation with human vision in medical image compression," *Med. Imaging Rev.*, vol. 14, no. 1, pp. 64–70, 2018. doi: 10.2174/1573405613666171003151036.
- [65] W. Yu, D. Hu, N. Tian, and Z. Zhou, "A novel search method based on artificial bee colony algorithm for block motion estimation," *EURASIP J. Image Video Process.*, vol. 2017, no. 66, pp. 1–14, 2017. doi: 10.1186/s13640-017-0214-1.
- [66] T. Bernatin and G. Sundari, "Comparitive analysis of different diamond search algorithms for block matching in motion estimation," *ARPJ. Eng. Appl. Sci.*, vol. 12, no. 11, pp. 3550–3553, 2017.
- [67] M. Jakubowski and G. Pastuszak, "Block-based motion estimation algorithms—A survey," *Opto–Electron. Rev.*, vol. 21, no. 1, pp. 86–102, 2013. doi: 10.2478/s11772-013-0071-0.
- [68] S. P. Metkar and S. N. Talbar, "Fast motion estimation using modified orthogonal search algorithm for video compression," *Signal, Image Video Process.*, vol. 4, no. 1, pp. 123–128, 2010. doi: 10.1007/s11760-009-0104-9.
- [69] J. M. Zain and M. Clarke, "Reversible region of non-interest (RONI) watermarking for authentication of DICOM images," *Int. J. Comput. Sci. Netw. Secur.*, vol. 7, no. 9, pp. 19–28, 2007.